Check for updates

Dual-locked spectroscopic probes for sensing and therapy

Luling Wu [1], Jiaguo Huang[2], Kanyi Pu [2] ✉ and Tony D. James [1,3] ✉

Abstract | Optical imaging probes allow us to detect and uncover the physiological and pathological functions of an analyte of interest at the molecular level in a non-invasive, longitudinal manner. By virtue of simplicity, low cost, high sensitivity, adaptation to automated analysis, capacity for spatially resolved imaging and diverse signal output modes, optical imaging probes have been widely applied in biology, physiology, pharmacology and medicine. To build a reliable and practically/clinically relevant probe, the design process often encompasses multidisciplinary themes, including chemistry, biology and medicine. Within the repertoire of probes, dual-locked systems are particularly interesting as a result of their ability to offer enhanced specificity and multiplex detection. In addition, chemiluminescence is a low-background, excitation-free optical modality and, thus, can be integrated into dual-locked systems, permitting crosstalk-free fluorescent and chemiluminescent detection of two distinct biomarkers. For many researchers, these dual-locked systems remain a 'black box'. Therefore, this Review aims to offer a 'beginner's guide' to such dual-locked systems, providing simple explanations on how they work, what they can do and where they have been applied, in order to help readers develop a deeper understanding of this rich area of research.

Optical imaging enables real-time, non-invasive detection of the localization, trafficking and activity of biomolecules in cells, tissues and even whole organisms with high spatiotemporal resolution and high sensitivity[1]. To correlate signal with molecular status or biological events in living systems, many 'always on' probes with the targeting or binding capability towards biomarkers have been developed[2]. However, as a result of nonspecific interactions, they have poor signal specificity and low signal-to-background ratio. By contrast, probes that are activated to fluoresce or chemiluminescence only after interaction with a biomarker of interest give rise to higher signal-to-background ratio and lower limit of detection, improving the performance of optical imaging for both in vitro and in vivo settings[3]. As such, the development of activatable probes has led to a better understanding and diagnosis of diseases such as cancer[4], neurodegenerative diseases[5], acute organ failure[6,7] and bacterial infection[8].

The construction of activatable probes requires multidisciplinary efforts that involve chemistry to design favourable fluorophore skeletons with 'off-on' properties, biology to validate molecular targets and detection ability, and medicine to evaluate diagnostic capability in preclinical and even clinical settings[9]. To date, a variety of activatable probes have been developed to detect metal ions[10], small signalling molecules[11], cellular

microenvironments[12,13], redox states and many other possible targets[11,14,15]. A general strategy is to conjugate an organic fluorophore or luminescent nanoparticle with a recognition moiety such that trapping or reacting with a specific biomarker or molecular event leads to the signal switching from an 'off' state to an 'on' state and, thus, indicates both the presence and the level of the biomarker[16]. However, such a one-to-one molecular design principle can still produce 'false positive' signals as a result of the difficulty posed by accurate recognition in complex biological milieu, because the undesired target sites often have moderate concentrations of biomarkers and the probe can be nonspecifically activated during transit[17]. In addition, single-locked probes are unable to detect two interlinked biomarkers or molecular events in targeted or diseases sites. Although coadministration of two different single-locked probes has the potential to simultaneously image two different biomarkers or molecular events, the different penetration capabilities, pharmacokinetics and metabolisms of single-locked probes can affect their behaviour and sensing ability in bioimaging applications.

The father of molecular logic, A. P. de Silva[18], has inspired numerous scientists to use logic-based approaches towards multianalyte sensing[19]. As molecular logic gates, dual-locked probes are able to respond to two different inputs with one or more outputs

[1]*Department of Chemistry, University of Bath, Bath, UK.*

[2]*School of Chemical and Biomedical Engineering, Nanyang Technological University, Singapore, Singapore.*

[3]*School of Chemistry and Chemical Engineering, Henan Normal University, Xinxiang, P. R. China.*

✉*e-mail: kypu@ntu.edu.sg; t.d.james@bath.ac.uk*

https://doi.org/10.1038/s41570-021-00277-2

(optical signals)[20]. For instance, a dual-locked probe might incorporate two responsive sites, allowing for dual stimuli (for example, two biomarkers or a biomarker combined with photoirradiation); they might also contain one responsive unit that undergoes a specific chemical change to expose a second responsive site. Thus, unimolecular dual-locked probes overcome many disadvantages of single-locked probes and display significantly reduced signal crosstalk and increased spatial resolution[21]. The ability to provide a response only when specific biomarkers are presented in a particular sequence can be especially important in the accurate monitoring of living organisms, producing specific signal output information as a result of intelligent recognition[22]. Furthermore, real-time simultaneous imaging of multiple biomarkers using unimolecular dual-locked probes enables investigation of the fundamental correlation between biomarkers and discrimination between them within pathological pathways in living organisms, but, perhaps more importantly, can also improve the accuracy of disease diagnosis[23].

In this Review, we summarize progress towards the development of dual-locked probes for bioimaging in living systems. We specifically focus on different chemical constructions that have been used to generate dual-locked probes with bespoke optical properties and to facilitate their specific activation towards different biomarkers. Our aim is to provide an overview of the tools and tactics currently available for detecting two biomarkers or one biomarker combined with another stimulus (such as photoirradiation) in biological environments using this dual-locked approach. Alongside this goal, we begin by describing different design strategies used in the construction of dual-locked probes and highlight a selection of representative examples for detecting biologically important biomolecules. We close with a discussion of current and future challenges in the field, with particular emphasis on the unmet needs for functional dual-locked probes.

Sequentially activated optical probes

In contrast to simple single-locked probes, dual-locked probes do not respond to a single biomarker. Rather, they are selectively activated by the correct combination and sequence of triggers. In this context, we highlight typical examples of dual-locked probes using a single optical channel (FIGS 1a,2a), exhibiting a sequential strategy for imaging and differentiation of biomarkers or biological events.

Near-infrared (NIR) light can interact with photosensitizers to generate singlet oxygen ($^1O_2$) from O_2, which can, in turn, react with chemiluminescent precursors, enabling chemiluminescence imaging[24]. Recently, probes **DCM-gal-CF** and **QM-B-CF** (FIG. 1b) were reported to facilitate bright chemiluminescence imaging of β-galactosidase and H_2O_2, respectively[25]. Specifically, the locking groups D-galactose and a boronated ester can be cleaved by β-galactosidase and H_2O_2, respectively, resulting in uncaged chemiluminescent precursors. Upon white light irradiation, the precursors can be oxidized to form the 1,2-dioxetane chemiluminescence substrate, followed by decomposition,

resulting in the emission of strong chemiluminescence signals. In addition to imaging, such sensing mechanisms have been expanded to include therapeutic function by Pu and colleagues[26]. **PEG-AE-5-DFUR** was composed of an adamantylidene enol ether conjugated with a chemotherapeutic 5′-deoxy-5-fluorouridine (5-DFU) using a H_2O_2 cleavable phenylboronic ester locking group (FIG. 1c). The prodrug (**PEG-AE-5-DFUR**) and a NIR photosensitizer (silicon 2,3-naphthalocyanine bis(trihexylsilyloxide)) were co-encapsulated into nanoparticles, affording **APtN**. Upon accumulation of **APtN** in the tumour of living mice following intravenous injection, the boronic ester locking group of **PEG-AE-5-DFUR** was specifically cleaved by the tumour-upregulated H_2O_2 to release 5DFUR. The uncaged adamantylidene enol ether could then react with $^1O_2$ produced by the photosensitizer upon laser irradiation of the tumours to afford the 1,2-dioxetane chemiluminescence substrate and, in turn, luminescence (FIGS 1d,e). Thus, in a locally controllable way, the theranostic responses are triggered by a cancer biomarker and the luminescence signals correlate with the drug release status.

Photocleavage induced by light has been applied as a trigger for dual-locked probes (probes **1–3**, FIG. 1f). A photoactivatable zinc probe **1** that contains a dichlorofluorescein scaffold functionalized with two di-(2-picolyl)amine receptors and two photocleavable *o*-nitrobenzyl groups was developed by Lippard and colleagues[27]. Upon ultraviolet (UV) light irradiation, photoinduced removal of the *o*-nitrobenzyl locking group restores the binding sites, allowing for zinc-responsive changes in fluorescence that could be observed in living HeLa cells and brain slices of mice. In addition, the enzyme-photoactivatable probes (**2** and **3**) are non-fluorescent xanthene derivatives owing to the locked diazoindanones and locking of the phenol or amine group with the acetyl or nitro groups, respectively[28,29]. Upon removal of the acetyl locking group by carboxylesterases or conversion of the nitro locking group into amine by nitroreductases, they become electron-rich and can undergo Wolff rearrangement under UV light irradiation. Thus, two sequential reactions of probes (**2** and **3**) produce bright rhodol and rhodamine analogues, enabling mapping of the subcellular distribution of enzymatic activity in live cells.

Sequentially activated dual-locked probes with two responses have received considerable attention because they can only be activated by the correct combination and sequence of triggers. Zhang and colleagues developed the probe **NML** that responds successively to the enzymes leucine aminopeptidase (LAP) and monoamine oxidase (MAO)[22], both of which are upregulated in diseases of the liver. **NML** contains a NIR hemicyanine dye linked to a 4-hydroxybenzyl and locked by a peptide-like receptor consisting of a leucine and a propylamine unit (FIG. 2b), and, as such, was initially non-fluorescent. The amide bond can be cleaved by LAP, and exposure of the resulting amine group to MAO leads to oxidation and β-elimination to release the fluorophore, resulting in a red shift of the absorption peak (FIG. 2c) and an appearance of strong emission at 720 nm. Importantly, **NML** is only fluorescence-activated in the presence of both LAP
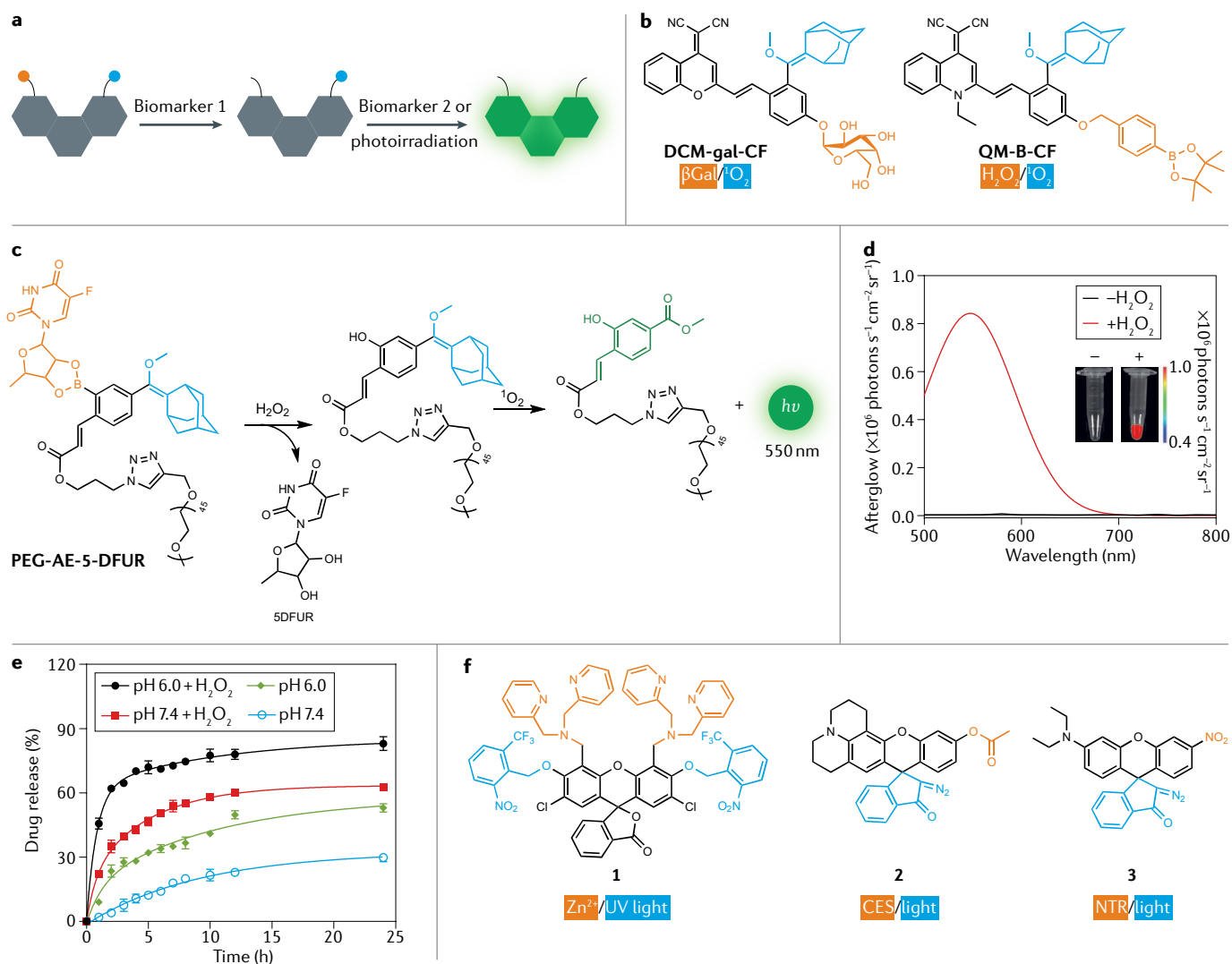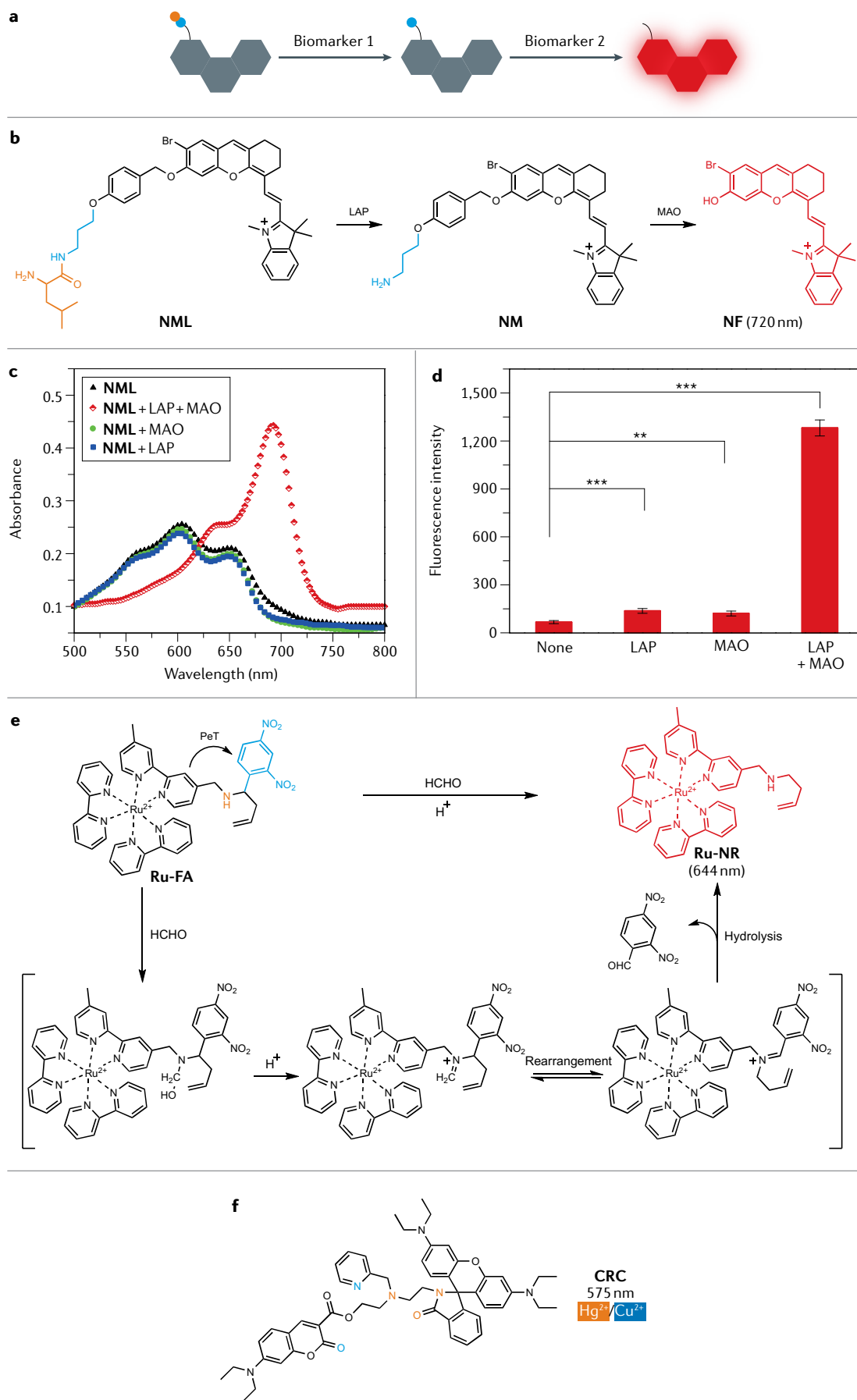
Fig. 1 | **Dual-locked probes containing two reaction sites that undergo two sequential reactions. a** | Schematic illustration of the concept. Two inputs, either two biomarkers or one biomarker combined with photoirradiation, lead to a turn-on of fluorescence output. **b** | Chemical structures of representative probes **DCM-gal-CF** and **QM-B-CF**. **c** | Chemical structures of a representative probe (**PEG-AE-5-DFUR**) and its activated forms in response to H_2O_2 and $^1O_2$. **d** | Luminescence spectra of **APtN** before and after activation. Inset: the corresponding images. **e** | 5DFUR release profiles of **APtN** in a tumour-microenvironment-mimicking acidic condition (pH = 6.0) and PBS (pH = 7.4) in the absence or presence of H_2O_2. **f** | Dual-locked probes that are activated by two independent reactions instigated by a biomarker and photoirradiation. The organic moieties that undergo the first reaction are shown in orange and the second in blue. βGal, β-galactosidase; CES, carboxylesterase; NTR, nitroreductase; UV, ultraviolet. Parts **d** and **e** reprinted with permission from REF.[26], Wiley.

and MAO but remains dark when just one of the enzymes is present (FIG. 2d). Such a cascade strategy requiring two inputs affords a lower background signal when each of the enzymes is only weakly expressed. This leads to greater accuracy for both in vivo imaging and in vitro serum testing to monitor drug-induced hepatopathy than single-response probes. In addition, **Ru-FA** was developed for the detection of lysosomal formaldehyde[30] (FIG. 2e). **Ru-FA** is non-fluorescent owing to a photoinduced electron transfer (PeT) process from the Ru(II) centre to 2,4-dinitrobenzene. Formaldehyde then triggers a 2-aza-Cope rearrangement reaction, resulting in a significant fluorescence enhancement at 644 nm. Excessive formaldehyde levels in tumours and successful NaHSO3 treatment to scavenge formaldehyde were confirmed using in vivo and ex vivo imaging. Another example is the highly selective coumarin–rhodamine conjugate (**CRC**) that could perform a sequential logic response to Hg^{2+} and Cu^{2+} (REF.[31]) (FIG. 2f). Only the addition of Hg^{2+} followed by Cu^{2+} results in noticeable fluorescence at 575 nm. When the order of addition is reversed, the probe was silent, as the binding strength of Hg^{2+} is insufficient to displace Cu^{2+}.

Signal activation and targeting

One potential issue with the aforementioned dual-locked probes is the relatively low spatiotemporal selectivity and specificity. Following reaction with the first biomarker,

a

b

c

d

e

f

◀ Fig. 2 | **Dual-locked probes containing one reaction site that undergoes two sequential reactions. a** | Schematic illustration of the concept. The first biomarker generates a non-fluorescent intermediate. Then, the further addition of second biomarker leads to a turn-on of fluorescence output. **b** | Chemical structures of a representative probe (**NML**) and its forms in response to leucine aminopeptidase (LAP) and monoamine oxidase (MAO). **c,d** | Normalized absorption spectra (panel **c**) and fluorescence response (panel **d**) of **NML** in the presence of LAP and/or MAO. **e,f** | Two examples of dual-locked probes that operate using two sequential reactions. CRC, coumarin–rhodamine conjugate; PeT, photoinduced electron transfer. Parts **c** and **d** adapted with permission from REF.[22], Royal Society of Chemistry (https://doi.org/10.1039/C9SC03628H).

the probe and the generated intermediate can diffuse and change location easily in highly heterogeneous and dynamic biological milieu. To improve the spatio-temporal selectively of dual-locked probes, one of the responsive sites can be a targeting unit, and the other site can then be responsible for producing an obvious signal enhancement (FIG. 3).

Tsien and colleagues have developed a genetically targeted calcium probe **Calcium Green FlAsH (CaGF)**[32]. **CaGF** contains two appropriately spaced trivalent arsenic, which can covalently bind with high selectivity to four cysteines at the i, $i+1$, $i+4$ and $i+5$ positions of a target protein[33,34]. Meanwhile, the o-aminophenol-N,N,O-triacetic acid (APTRA) amidated with morpholine serves as a calcium ion (Ca^{2+}) receptor that exhibits high selectivity over magnesium ion (Mg^{2+}) (FIG. 3b). Using this system, a fourfold increase in fluorescence intensity was observed when **CaGF** binds to a tetra cysteine protein motif, and the sequential addition of Ca^{2+} results in an additional tenfold fluorescence enhancement. **CaGF** was used to anchor tetra-cysteine-tagged connexin 43 and monitor Ca^{2+} waves through gap junctions in HeLa cells. In a similar fashion, the Rao group has used a fluorescein derivative as fluorescent reporter to develop a dual-locked probe for imaging *Mycobacterium tuberculosis* (*Mtb*)[35]. With this system, **CDG-Tre** was activated by β-lactamase (BlaC) to generate fluorescent 6-TG-Tre (FIG. 3c). The fluorescent 6-TG-Tre is then linked by antigen 85 (Ag85) enzymes into 6-TG-Tre-MM, which is incorporated into the cell wall and stains the bacteria. **CDG-DNBs** developed by Rao and colleagues represents another example of dual-locked probes for *Mtb*[36]. Reaction of **CDG-DNBs** with BlaC forms fluorescent Fluoro-DNB, which is then covalently linked to the decaprenylphosphoryl-β-D-ribose 2′-epimerase (DprE1) of *Mtb* (FIG. 3d). Another strategy, developed by Vendrell, Kitamura and colleagues, uses specific binding interactions and changes in pH of tissue microenvironments. The **mCCL2-MAF** probe ($pK_a \sim 4.9$) contains a pH-dependent BODIPY and a CCR2 ligand (mouse chemokine CCL2)[37]. The fluorescence signal ($\lambda_{em} = 510\,nm$) of **mCCL2-MAF** was activated through macrophage chemokine receptor CCR2-mediated internalization and phagosomal acidification-induced protonation. As such, **mCCL2-MAF** could selectively stain metastasis-associated macrophages in tumours of a mouse model after intravenous injection, but did not label neutrophils, natural killer cells, T cells or B cells.

Probing with two independent optical channels

Real-time simultaneous imaging of multiple biomarkers can facilitate both the fundamental correlation between different biomarkers in a certain pathological pathway and improving the accuracy of disease diagnosis[21]. However, many activatable probes are generally functionalized with a single reaction site and, thus, only able to respond to a single biomarker. Although such a dual response might be achieved by the coadministration of two or more different probes, such procedures are particularly complicated. Accurate correlations between signals (and, thus, biomarkers) are difficult to show convincingly, as a result of variations in cellular uptake, site distribution within the cell and in vivo pharmacokinetics between probes, as well as possible signal crosstalk. By contrast, dual-locked probes with two optical channels can overcome these difficulties (FIGS. 4,5). Several examples of this approach have proved fruitful for the monitoring of two cascade biomarkers or the discrimination of two different biomarkers.

Transformations between various reactive oxygen species (ROS) often occur in living systems, for example, production of H_2O_2 from $O_2^{\bullet-}$ by superoxide dismutase and conversion of H_2O_2 into HClO by myeloperoxidase[11,38]. As such, real-time imaging and discrimination of ROS in living systems is essential to understand their individual functions and correlations. Probe **FHZ** was developed by the reconstruction of a fluorescein molecule for the discrimination of $^{\bullet}$OH and HClO (REF.[39]) (FIG. 4b). The parent probe molecule is non-fluorescent, as the five-membered ring interrupts the conjugation, reducing the electron delocalization in the latent fluorescein. The sensing mechanisms for ROS discrimination rely on the different oxidative reactivity of $^{\bullet}$OH and HClO; specifically, $^{\bullet}$OH is a much stronger oxidant than HClO. Thus, in the presence of HClO, the five-membered ring alone is opened through a sequence of addition and elimination reactions to yield product **F-TEG** with strong green fluorescence (FIG. 4c). In the presence of $^{\bullet}$OH, however, the bottom-left aromatic ring is oxidized and opened, producing **FOBA** with strong cyan fluorescence (FIG. 4d). Although many ROS have only short lifetimes, the distributions of spontaneously produced $^{\bullet}$OH and HClO in living zebrafish were simultaneously visualized and discriminated using **FHZ**.

Independent response strategies have also been used to detect both biomarkers (e.g. thiols) and changes in the biological environment (e.g. intracellular viscosity). For example, Ma, Li, Lin and colleagues have synthesized probes to monitor both variations of intracellular viscosity and changes in $^{\bullet}$OH, H_2S, as well as H_2O_2, in living cells (FIG. 4e). The sensing mechanisms rely on the restriction of intramolecular rotation (viscosity) and oxidative or reductive cleavage reactions[40–42]. p-Thiocresol and 2,4-dinitrobenzenesulfonyl moieties are commonly used as protecting (locking) groups that can be removed (unlocked) by nucleophilic aromatic substitution reactions with nucleophilic thiols. The discrimination of glutathione (GSH) from cysteine/homocysteine using probe **S-S-BODIPY-S**, the monitoring of cysteine metabolism using **4** and the detection of biothiols and SO_2
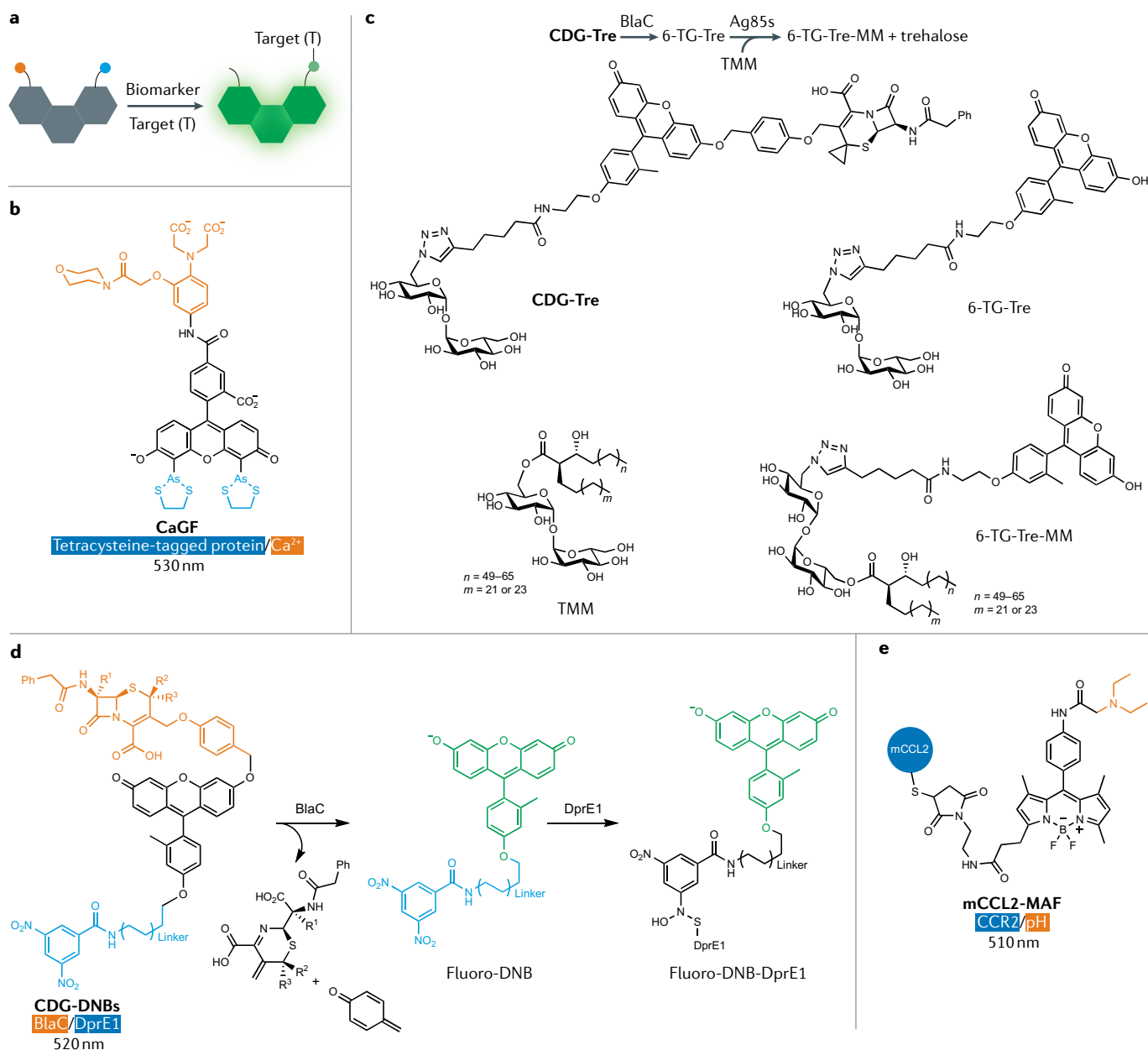
Fig. 3 | **Dual-locked probes containing two reaction sites enabling signal activation and targeting. a** | Schematic illustration of the concept. One reaction site is used to generate a significant turn-on fluorescence output and the other is for specific protein/organelle targeting. **b** | Chemical structure of a representative probe (**CaGF**). **c** | Probe **CDG-Tre** activated by β-lactamase (BlaC) to give 6-TG-Tre, which was processed by Ag85 enzymes into 6-TG-Tre monomycolate (6-TG-Tre-MM) via mycolate chain transfer from another molecule of trehalose monomycolate (TMM). 6-TG-Tre-MM could then be incorporated into the bacterial cell wall. **d** | Structure of dual-targeting fluorogenic probes (**CDG-DNBs**) and reaction with BlaC and decaprenylphosphoryl-β-D-ribose 2′-epimerase (DprE1). **e** | Structure of dual-locked probe **mCCL2-MAF**.

using **BPO-Py-diNO₂** have been investigated in a fluorometric manner[43–45] (FIG. 4e).

Simultaneous monitoring of two caspase cascade activation processes in living cells has been studied by using aggregation-induced emission (AIE) probe **5** (REF.[46]) (FIG. 5e). Two AIE fluorogens (red tetraphenylethylene-thiophene and green tetraphenylsilole) were connected to opposite ends of a hydrophilic peptide conjugate (DVEDIETD), which is, itself, composed of two short peptides, DVED and IETD, which are, respectively,

the substrates for the effector caspase 3 and the apoptosis initiator caspase 8. In aqueous media containing DMSO, the AIE probe was initially non-fluorescent. However, in apoptotic HeLa cells, green and red fluorescence could be activated when the peptide substrate was cleaved through cascade activation by caspase 8 and caspase 3, respectively. In addition, the two-photon fluorescence-lifetime-based probe (**TFP**) was developed for the imaging of mitochondrial H_2O_2 and adenosine 5′-triphosphate (ATP) changes in living cells[47] (FIG. 5e–g).

Although the dual-locked probes discussed in this section can produce two fluorescence outputs, signal crosstalk often occurs as a result of overlap in the emission spectra, thus compromising the sensitivity of detection. Integration of fluorescence and chemiluminescence signals into one system is an emerging approach to avoid signal crosstalk, providing a transformative approach for imaging applications[21]. Pu and colleagues have reported a highly renal-clearable activatable duplex reporter (**ADR**) for the chemiluminescent and NIR fluorescence imaging of contrast-induced acute kidney injury in a murine model[21]. Both $O_2^{\bullet-}$ and lysosomal enzyme *N*-acetyl-β-D-glucosaminidase (NAG) are upregulated in renal tubular cells in the course of this disease. **ADR** was designed using an $O_2^{\bullet-}$-activatable chemiluminescent unit and a NAG-activatable NIR fluorescence moiety, both of which were linked to a renal-clearance scaffold, (2-hydroxypropyl)-β-cyclodextrin (FIG. 5b). **ADR** was initially non-fluorescent and non-chemiluminescent, as both of the luminophores were in 'caged' states. In the presence of NAG, cleavage of the glycosidic bond

led to the formation of uncaged fluorophore with strong fluorescence at 720 nm (FIG. 5c). Meanwhile, $O_2^{\bullet-}$ attacks the triflyl, resulting in deprotection. The resultant uncaged dioxetane is unstable and undergoes decomposition to release a chemiluminescence signal (FIG. 5d). After systemic administration of **ADR** into living mice, it produced chemiluminescence and NIR fluorescence signals that report on the $O_2^{\bullet-}$ and NAG levels, respectively, in the kidneys. This independent dual-locked sensing capability of **ADR** avoids any signal crosstalk, resulting in the detection of contrast-induced acute kidney injury prior to clinical and preclinical assays. In parallel with this study, the Pu group has developed another chemo-fluoro-luminescent probe (**CFR**, FIG. 5e) for crosstalk-free duplex imaging of $O_2^{\bullet-}$ and caspase 3 using a mouse model of drug-induced liver injury[23], while Rao and colleagues have developed a nanoprobe for the fluorescence and chemiluminescence imaging of ROS and reactive nitrogen species in a mouse model for drug-induced acute hepatotoxicity[48].
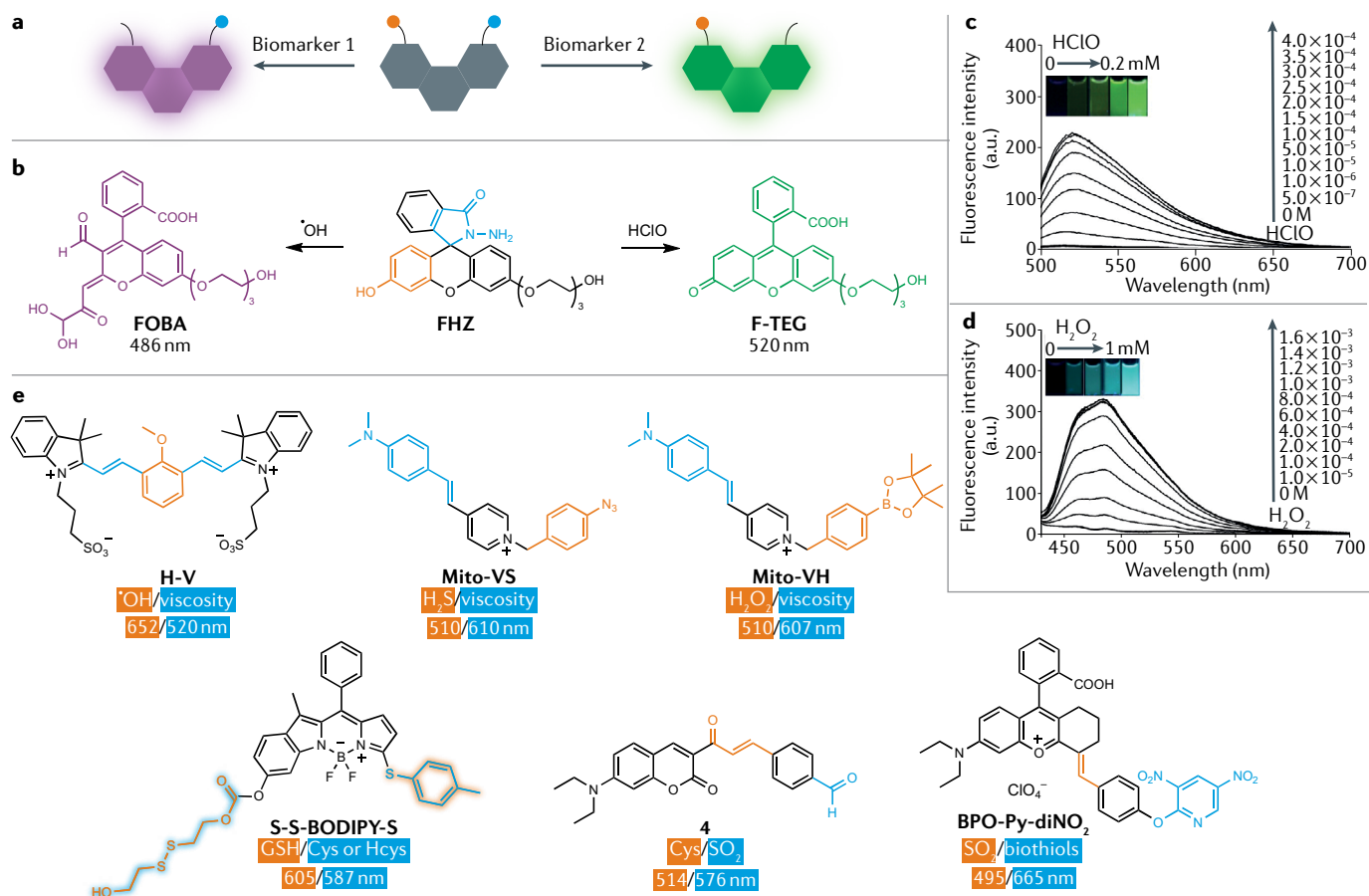

Fig. 4 | **Dual-locked probes containing one fluorophore that can undergo two independent reactions. a** | Schematic illustration of the concept. Two biomarkers lead to two independent turn-ons of fluorescence outputs. **b** | Chemical structures of a representative probe (**FHZ**) and its activated forms in response to ˙OH and HClO, respectively. **c** | Fluorescence response of **FHZ** in the absence or presence of different equivalents of HClO. **d** | Fluorescence response of **FHZ** in the absence or presence of different equivalents of ˙OH. ˙OH is formed by Fenton reaction between $FeSO_4$ and H_2O_2. **e** | Dual-locked probes based on one fluorophore. The organic moieties that respond to different biomarkers are in orange and blue. The organic moieties that can respond to both orange and blue biomarkers are in orange/blue and blue/orange. Cys, cysteine; GSH, glutathione; Hcys, homocysteine. Parts **c** and **d** reprinted with permission from REF.[39], ACS.

Fluorescent 'AND'-based probes

In general, 'AND'-based systems require the simultaneous coexistence of two analytes to obtain a significant fluorescence enhancement. Such duplex-responsive probes provide numerous advantages when compared with single-analyte probes, including the following: (1) they produce a significant 'turn-on' fluorescence response via the removal of dual-locked quenching groups and (2) they provide a method to investigate the cooperative relationship between two analytes[49].

As discussed above, these dual-locked probes can produce a fluorescent 'on' state when two analytes are added in a specific sequence. Although some groups have developed dual-locked systems using sequential AND logic[22,25,27], here, we discuss AND-based probes that can be activated and produce a strong fluorescence emission output, irrespective of the sequence of analyte addition (FIG. 6a). Such probes containing dual-locked sites require the coexistence of both analytes to produce a fluorescence response, and reaction at just one locking site results in a negligible response[11]. One good example is **GSH-PF3**, which was synthesized by attaching boronic acid pinacol ester and 2,4-dinitrobenzenesulfonyl (locking sites for ONOO⁻ and GSH, respectively) to a fluorescein core[50] (FIG. 6d). The addition of just ONOO⁻ or GSH produced minimal fluorescence response, while a significant enhancement (40-fold) was observed when both are present, regardless of the addition sequence. As such, it was feasible to use **GSH-PF3** to visualize the dynamic coexistence of ONOO⁻ and GSH by fluorescence imaging in RAW264.7 cells. This was achieved using lipopolysaccharide stimulation (which produces ONOO⁻) and caffeic acid treatment (an anti-inflammatory drug that stimulates the cellular production of GSH). Subsequently, 4-amino-2-(benzo[d]thiazol-2-yl)phenol was used as a fluorophore in the development of the probe **GSH-ABAH**[51] (FIG. 6d). The dual-locked probe **GSH-ABAH** contains two reaction sites: one is a locked excited-state intramolecular proton transfer (ESIPT) fluorophore for ONOO⁻ and the other a PeT site that deactivates on reaction with GSH. Similarly, the pinkment systems, **Pinkment-OTBS** and **Pinkment-OAc**, based on the resorufin fluorophore, have been used to monitor the reactive oxygen and nitrogen species AND F⁻ or ROS AND esterase, respectively[52] (FIG. 6d).

It is well known that the inclusion of electron donating groups at the 7-position of coumarin can enhance its fluorescence intensity[53]. Zhou and Fahrni have exploited this to demonstrate that the formation of an electron donating triazole can lead to a significant 'turn-on' fluorescence when introduced by means of a Cu(I)-catalysed azide–alkyne cycloaddition reaction[54]. A maleic acid monoamide unit appended at the 3-position of the coumarin quenches the fluorescence through the PeT process. Thus, in the dual-locked probe **C1** (FIG. 6b,c), the fluorescence is turned on only by the combination of triazole formation and deactivation of the quenching unit[55].

Li, Yi, Xi and colleagues have developed an AND-logic-based system to investigate the relationship between hydrogen sulfide (H_2S) and human NAD(P)H:quinine oxidoreductase 1 (hNQO1) in cellular redox homeostasis[49]. Probes **6** and **7** (FIG. 6d) combine PeT quenching units and Förster resonance energy transfer (FRET), and are based on coumarin and naphthalimide fluorophores, respectively. 7-Nitro-1,2,3-benzoxadiazole amines[56] and quinone propionic acid[57] serve as the reaction sites for H_2S and hNQO1, respectively. Probes **6** and **7** exhibited a strong fluorescence enhancement when exposed to H_2S and hNQO1 simultaneously. However, probe **7** exhibited a larger 'turn-on' (>400-fold) than probe **6** (220-fold) when exposed to the two biomarkers. Probe **7** facilitated the differentiation of enhanced concentrations of endogenous H_2S and hNQO1 in HT29 and HepG2 cells from FHC, HCT116 and HeLa cells. Therefore, dual-locked probe **7** permitted visualization of the collaborative antioxidant effects of H_2S and hNQO1 in response to oxidative stress in HeLa cells.

The dual-locked AND systems described above are examples of single probes using one fluorophore. However, there is a further design strategy in which two probes react with two analytes, and then the generated species undergo further reaction to form a luminescent species. Chang and colleagues took advantage of the bioluminescent probe **PCL-1** for the detection and imaging of H_2O_2 (REF.[58]). They subsequently developed **PCL-2**, in which a self-immolative benzylic linker can be removed when H_2O_2 triggers cleavage of the boronic acid to generate 6-hydroxy-2-cyanobenzothiazole (HCBT). Meanwhile, reaction of the pentapeptide probe **z-Ile-Glu-ThrAsp-D-Cys** (**IETDC**) with caspase 8 releases D-Cys, which undergoes a cyclization reaction with HCBT to form firefly luciferin. The product of this cyclization is then further catalysed by firefly luciferase to produce a bioluminescent signal[59] (FIG. 7). The single-locked probe **PCL-2** and the **IETDC** peptide can be used to monitor changes in the endogenous levels of H_2O_2 and caspase 8 activity, respectively. Importantly, the combination of **PCL-2** and **IETDC** was validated for the simultaneous detection of both bioanalytes in a mouse model of inflammatory disease.

FRET-based probes

FRET is a photochemical process in which energy transfer occurs from a donor in its excited state to an acceptor in its ground state. When both the donor and the acceptor are fluorophores, FRET is termed fluorescence (instead of Förster) resonance energy transfer.
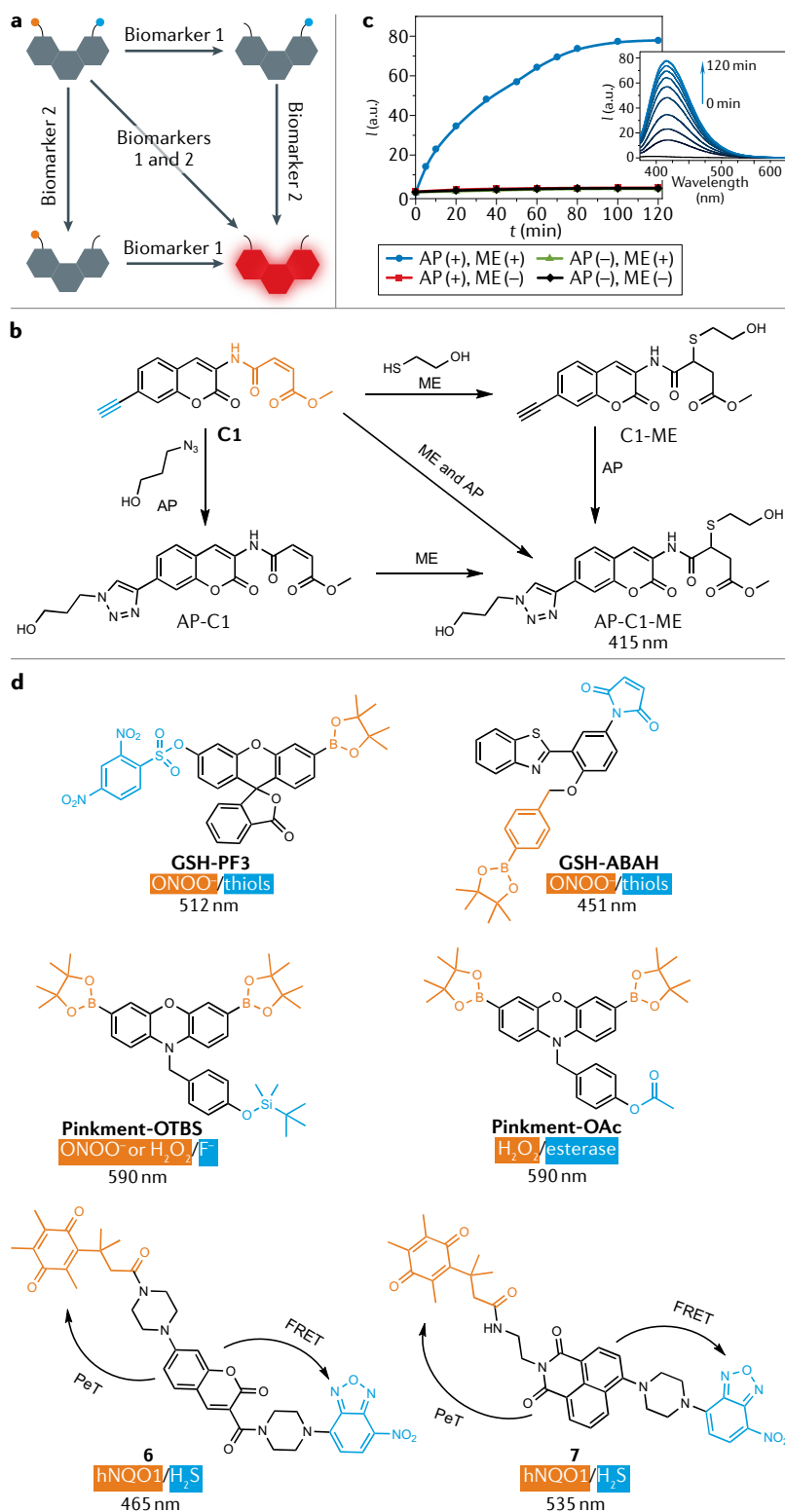
Various FRET-based fluorescent probes have been developed for the detection and imaging of biological species (for example, cations or anions) or monitoring of the biological environment (for example, pH or hypoxia)[60]. This section includes some representative fluorescent probes using the FRET fluorescence mechanism as a strategy for the detection of two analytes.

The most commonly described type of dual-locked FRET-based probe incorporates both a FRET donor and a FRET acceptor, as shown in FIG. 8a. Such probes exhibit short-wavelength fluorescence emission (green), i.e. directly from the FRET donor, after reaction of the system with the first analyte. A long-wavelength fluorescence emission (red), i.e. from the FRET acceptor, is obtained only when the second analyte is present. These two processes are similar to the mechanism outlined in FIG. 5. In this case, however, a red fluorescent output is obtained whenever both analytes are present (irrespective of the sequence of addition). A very recent review has covered such probes (**FP-H₂O₂-NO**, **N₃-CR-PO₄**, **Naph-RhB** and **DDP-1**)[60–64]. As such, here, we discuss another dual-locked system using the FRET fluorescence mechanism (FIG. 8b).

Heatstroke (HS) is a heat-related pathology that induces a number of intercellular processes (e.g. metabolic disorders and apoptosis). However, there is a lack of understanding of the molecular and organelle-related mechanisms occurring during the process of HS[65]. The relationship between temperature and SO_2 concentration in lysosomes remains uncertain. As such, Yin and colleagues have developed photoactivated probe **Ly-NT-SP** for SO_2 (REF.[66]) (FIG. 8c,d). The morpholine group of **Ly-NT-SP** facilitates its accumulation in lysosomes. Upon UV irradiation, the spiropyran ring is opened to form a hemicyanine; the increased spectral overlap between the emission of the naphthalimide and the absorption of the hemicyanine leads to FRET. However, SO_2 is a nucleophile that can react by addition to the 'unlocked' C=C double bond of the hemicyanine, interrupting the π-conjunction and inhibiting the FRET process. Using the **Ly-NT-SP** system, an increase in temperature was shown to result in an increase of lysosomal SO_2 levels. Additionally, dual-channel tissue imaging based on **Ly-NT-SP** indicated that SO_2 could reduce small intestinal damage by scavenging ROS induced by HS[66].

Other dual-locked probes

In this section, we discuss probes with two locked/reaction sites that are initially non-fluorescent (FIG. 9a). Fluorescence emission results from the presence of a specific analyte; however, the fluorescence emission wavelength shifts (either red-shifted or blue-shifted) when the second analyte is introduced. This phenomenon can only be observed when the two analytes trigger their reactions in a specific sequence. ESIPT fluorophores are sensitive to the surrounding environment as a result of a rapid four-level photochemical process[67]. The first level of an ESIPT fluorophore is the ground state of the enol (E(S_0)). Excitation to the first excited singlet state of the enol (second level or E*(S_1)) leads to conversion into the corresponding first excited singlet state of the
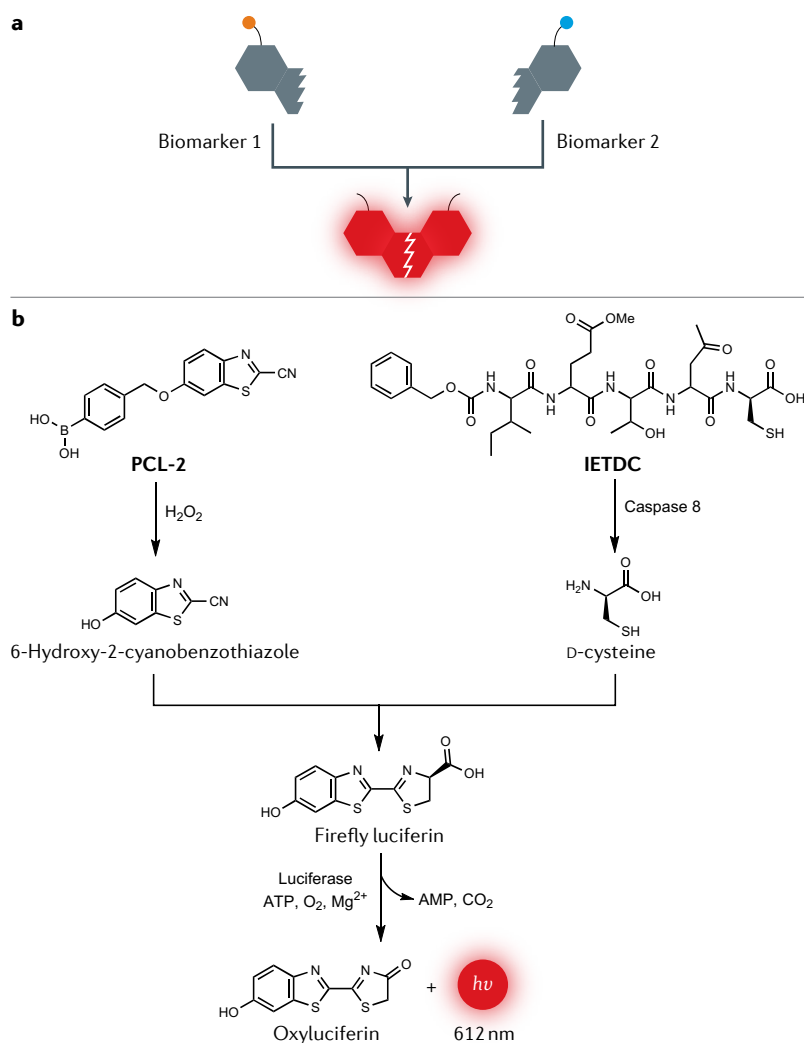
Fig. 6 | **AND-logic-based unimolecular fluorogenic probes. a** | Schematic illustration of the concept. A fluorescent dye is dual-locked by two functional groups, which respond to two different analytes. The fluorogenic probe requires both analytes to be present or to work in tandem in order to produce a response. **b,c** | Probe **C1** for the detection of AP AND ME. **d** | Other AND-logic-based probes using different fluorophores. The organic moieties that undergo the two responses are in orange and in blue. AP, 3-azido-1-propanol; FRET, Förster resonance energy transfer; GSH, glutathione; ME, 2-mercaptoethanol; PeT, photoinduced electron transfer. Part **c** adapted with permission from REF.[55], Wiley.

Fig. 7 | **AND-logic-based system using two precursor probes. a** | Schematic illustration of the concept. Two biomarkers react with the corresponding precursor probes to form two intermediates, which undergo further reaction to generate a turn-on bioluminescence output. **b** | Design strategy for simultaneous detection of H_2O_2 and caspase 8 activity through release of 6-hydroxy-2-cyanobenzothiazole and D-cysteine, and in situ formation of firefly luciferin. AMP, adenosine monophosphate; ATP, adenosine 5′-triphosphate.

keto form (third level or $K^*(S_1)$). A longer wavelength emission is then produced when electrons from the keto form in the $K^*(S_1)$ excited state return to the fourth level and ground state of the keto form (i.e. $K(S_0)$). The ESIPT-based probe **3-HF-OMe** was constructed by combining the 3-hydroxyflavone (3-HF) fluorophore and ONOO−-responsive boronate unit. **3-HF-OMe** binds as a 'guest' molecule within the hydrophobic cavity of a 'host' matrix of amyloid-β (Aβ) peptide aggregates. The hydrophobic environment leads to an enhanced fluorescence emission at 420 nm of probe **3-HF-OMe** (REFS[68,69]). Then, addition of ONOO− activates the photo-tautomeric fluorescence state of the ESIPT fluorophore, resulting in a new emission at 520 nm (REF.[70]) (FIG. 9b,d).

Probe **HCy-FN** is capable of differentiating $O_2^{\bullet-}$ and H_2S_n, producing emissions at 794 and 625 nm, respectively[71] (FIG. 9c). Initially, **HCy-FN** was non-fluorescent. Then, a hydrogen abstraction reaction by $O_2^{\bullet-}$ facilitates the D-π-A conjunction of **Cy-FN**,

resulting in emission at 794 nm. Subsequent attack by the H_2S_n on **Cy-FN** results in two nucleophilic substitutions to generate **Keto-Cy** with blue-shifted emission at 625 nm. The initial displacement of the F− of **Cy-FN** by H_2S_n is an S_NAr reaction, which forms an intermediate containing a free −SH group, which subsequently undergoes intramolecular cyclization to release **Keto-Cy** (REFS[71–73]).

Acidic pH and overexpression of GSH are hallmarks of cancer[74,75]. Guo, Zhu and colleagues have developed a prodrug **P(Cy-S-CPT)**, where the active anticancer drug camptothecin (CPT) is released by sequential stimulation acid and GSH (REF.[76]) (FIG. 9e). At neutral pH (7.4), aggregation of the amphiphilic diblock copolymer of the nanoprobe **P(Cy-S-CPT)** leads to the formation of spherical micelles. As a result, the NIR fluorescent component **Cy-S-CPT** becomes concentrated within the hydrophobic core of the micelle, resulting in a significant quenching of fluorescence at 830 nm. The formation of micelles also prevents the release of drug because it is protected from nucleophilic attack by GSH within the hydrophobic core. Lowering the pH (to a value below the pK_a) leads to protonation of the tertiary amine. This enhances the hydrophilic nature of **P(Cy-S-CPT)**, resulting in disassembly of the micelle and a fluorescence increase at 830 nm. The dissembled **P(Cy-S-CPT)** is then readily attacked by GSH, triggering the release of CPT in synergy with a remarkably blue-shifted fluorescence emission from 830 to 650 nm. Therefore, this two-biomarker logic-based probe not only provides a model for monitoring drug release but also facilitates targeted drug delivery.

Next, we discuss the dual-locked probes where one reaction site can generate two different fluorescence emissions in response to two analytes, dependent on the addition sequence (FIG. 10a). The o-phenylenediamino moiety is a common recognition motif for nitric oxide (NO). It reacts with NO+ or N_2O_3 to irreversibly generate benzotriazole derivatives[77,78], resulting in fluorescence 'turn-on' as PeT quenching is inhibited[78,79]. Probe **8** was constructed by incorporating the o-phenylenediamino group at the 9-position of a pyronin dye[80] (FIG. 10b). Conjugation between the fluorophore and one amino unit of o-phenylenediamino provides three main benefits: (1) minimized interference from ascorbic acid, dehydroascorbic acid[81,82] and methylglyoxal[83]; (2) stable fluorescence of probe **9** over a pH range from 7 to 8, as the benzotriazole product is insensitive to pH (REFS[77,78]); and (3) facilitated accumulation of probe **8** in mitochondria, as a result of its positive charge. Treatment of probe **8** with GSH or Cys did not lead to a fluorescence output. However, a noticeable fluorescence enhancement at 616 nm was observed when probe **8** was exposed to diethylamine NONOate diethylammonium salt (a NO donor), as a result of the formation of compound **9**. Benzotriazole can serve as a leaving group in S-acylation reactions[84], and, as a result, the benzotriazole of **9** underwent an S_NAr substitution–rearrangement reaction when treated with Cys, leading to formation of dye **11** (via intermediate **10**), with an enhancement in emission at 536 nm. In addition, a simple S_NAr substitution between compound **9** and GSH generates fluorescent **12**,
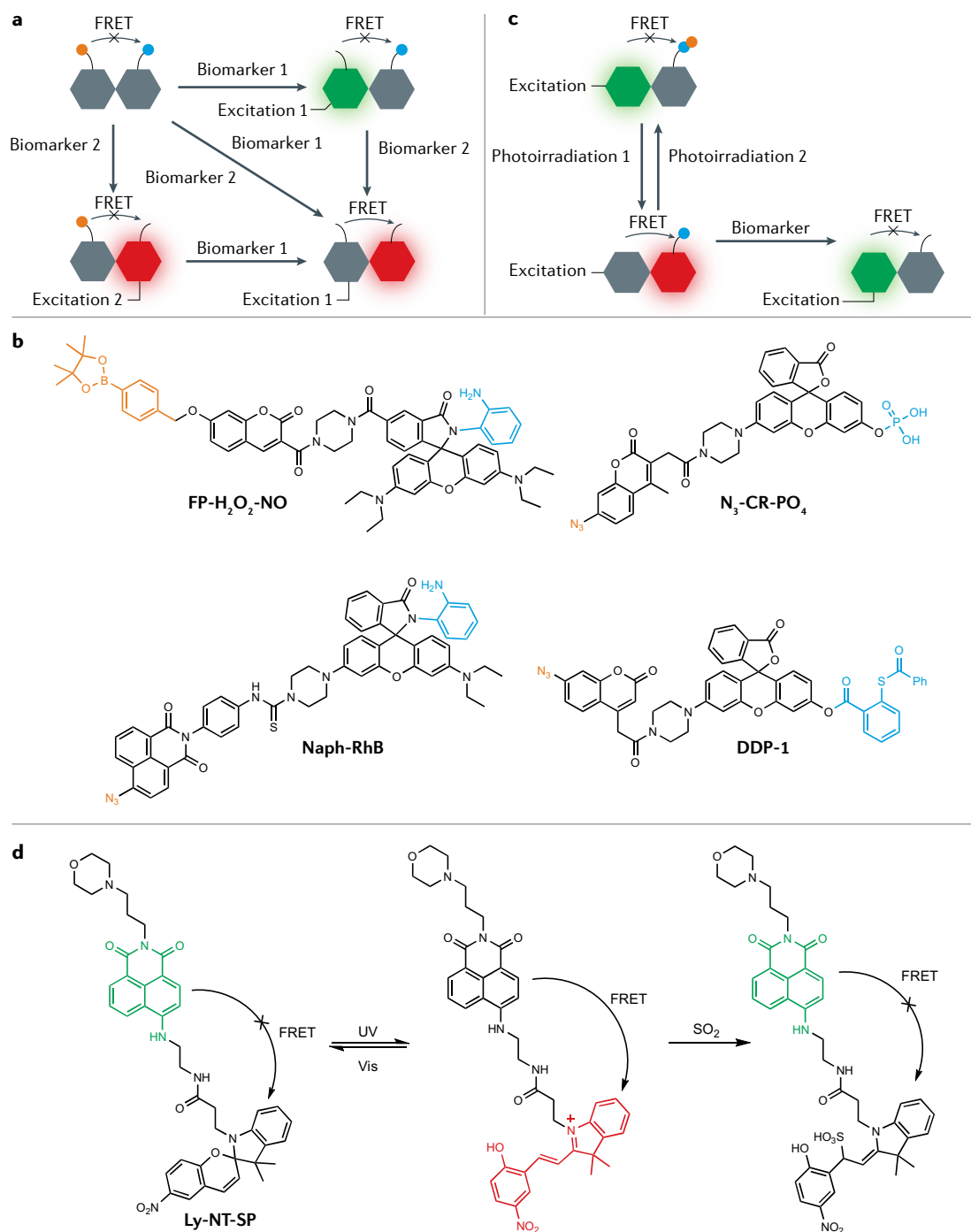
Fig. 8 | **Förster resonance energy transfer in the construction of dual-locked fluorescent probes. a** | Design concept for a Förster resonance energy transfer (FRET)-based system using two fluorophores and two responsive sites. One biomarker leads to a turn-on fluorescence output and no FRET occurs. Both biomarkers lead to FRET; therefore, the probes exhibit longer emission using short excitation wavelengths. **b** | Dual-locked probes that operate based on the type of FRET illustrated in panel **a**. The organic moieties that behave as the responsive sites are in orange and in blue. **c** | Design concept for a FRET-based dual-locked probe containing one responsive unit. Photoirradiation of the probe generates a FRET acceptor. The process can be reversed when the FRET acceptor is irradiated using light of a different wavelength. Subsequent addition of a biomarker alters the conjugation of the acceptor and inhibits the FRET process. **d** | Molecular design of **Ly-NT-SP** and proposed sensing mechanism towards SO_2. UV, ultraviolet; Vis, visible.

which exhibited emission at 618 nm. Coumarin-based photo-triggers have been widely used for the development of photo-responsive systems, as a result of their strong fluorescence and efficient photo-release capability[85]. Coumarin-based non-fluorescent prodrug **13** is unlocked only by the presence of two 'keys' in the correct sequence. The first key is hypoxia, which leads to reduction of the nitro group (the first lock) and
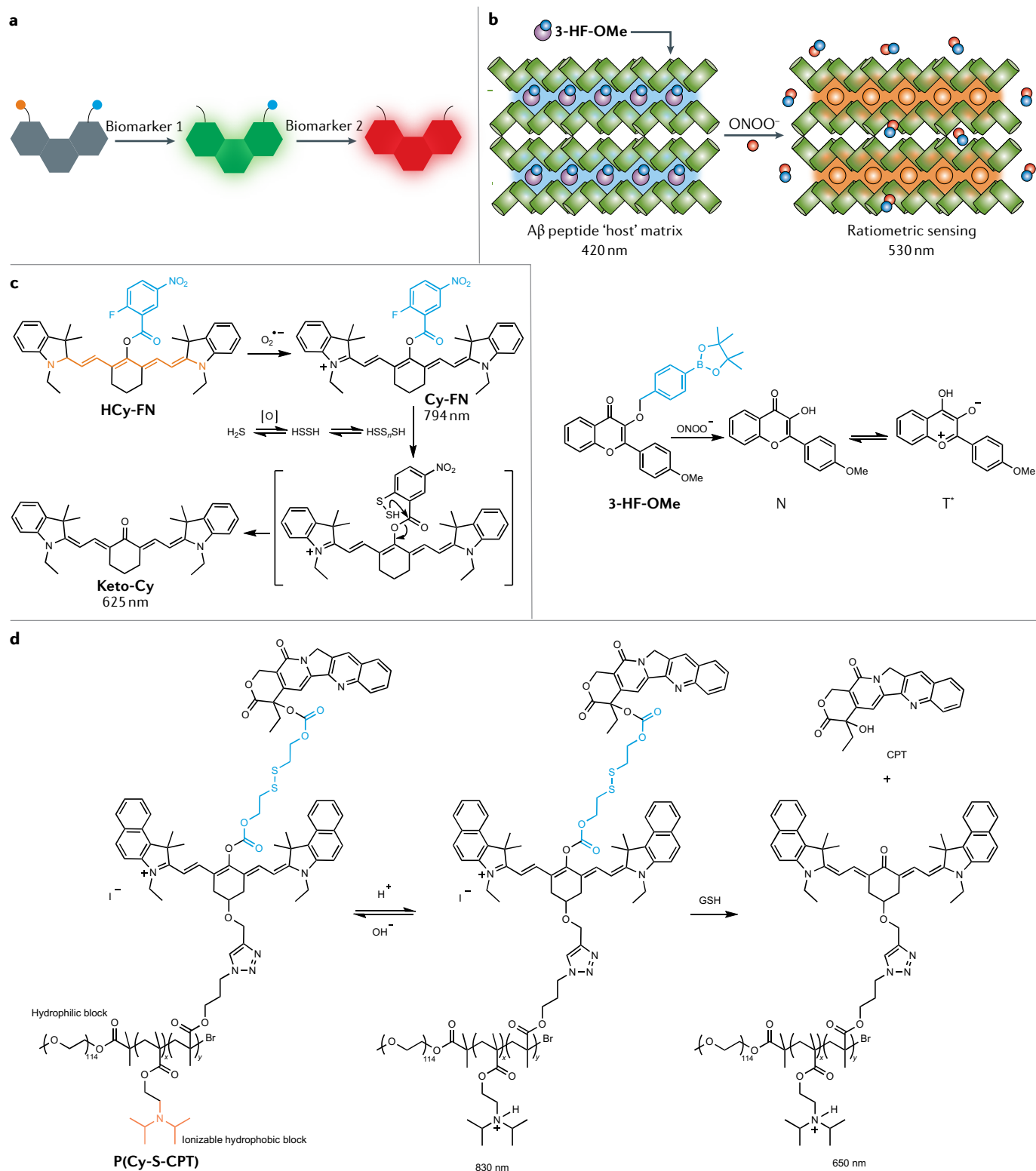
Fig. 9 | **Sequential addition of two analytes to induce two different fluorescence channels in a dual-locked system.** **a** | Schematic illustration of the concept. The first biomarker induces a turn-on fluorescence signal and the second biomarker results in a blue or red shift in emission. **b** | Schematic illustration of the proposed interactions of probe **3-HF-OMe** with amyloid-β (Aβ) aggregates and their use as a new host–guest system for the ratiometric sensing of peroxynitrite (ONOO⁻). **c** | Proposed reaction mechanism of probe **HCy-FN** for O$_2$$^{•-}$ and H$_2$S$_n$ detection. **d** | Design of a sequence-activated dual-channel near-infrared theranostic nanoprodrug. CPT, camptothecin; GSH, glutathione. Panel **b** adapted with permission from REF.[70], ACS (https://pubs.acs.org/doi/10.1021/jacs.8b08457); further permissions related to the material excerpted should be directed to the ACS.
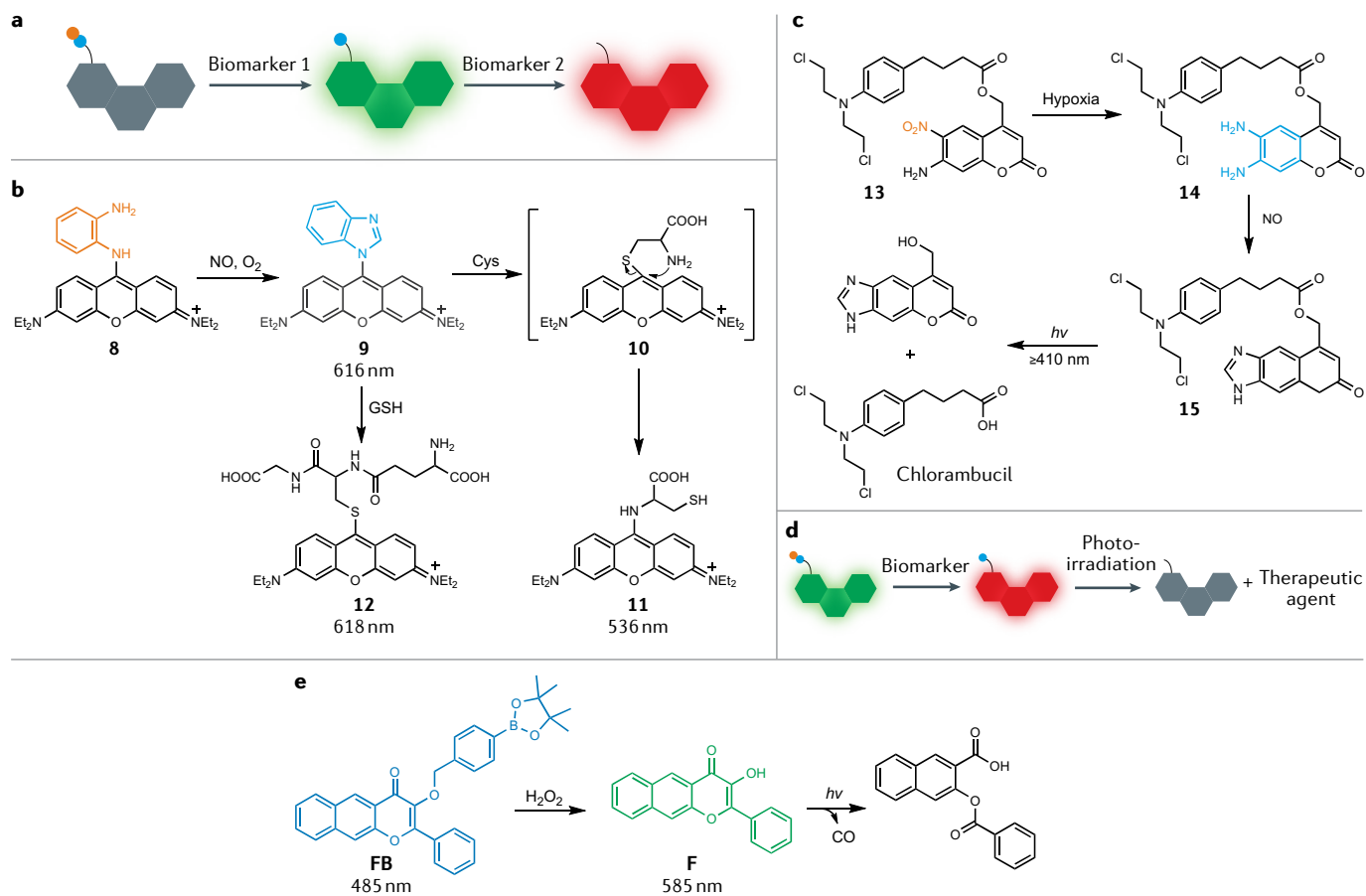
Fig. 10 | **Other types of dual-locked fluorescent probes. a** | Schematic illustration of non-fluorescent dual-locked probes with one reaction site that can generate two different fluorescence signals. The first biomarker leads to exposure of the second reaction site. **b** | Proposed reaction mechanisms of **8** with NO in the presence of cysteine (Cys) and glutathione (GSH), respectively. **c** | Working protocol of dual-locked probe **13** towards hypoxia and NO with chlorambucil release. **d** | Schematic illustration of a fluorescent dual-locked probe with one reaction site that can generate a fluorescent intermediate and then, under photoirradiation, produce a non-fluorescent product with the release of a therapeutic agent. **e** | The chemical structure of **FB** and the corresponding CO photo-release mechanism.

formation of *o*-phenylenediamino unit, resulting in green fluorescence emission. Subsequent addition of NO (the second key) generates the electron-deficient triazole of compound **15** with a blue fluorescence emission[86] (FIG. 10c). The drug chlorambucil attached to compound **15** can be released under irradiation with visible light (≥410 nm), and, thus, prodrug **13** can also be described as a triple-locked probe.

The final type of dual-locked probes is displayed in FIG. 10d, where a red shift occurs when the probe is first activated by a specific biomarker. Subsequent stimulation using photoirradiation induces decomposition of the intermediate and release of a therapeutic agent. A representative example is prodrug **FB**, a two-photon flavonol–borate-based fluorescent probe with maximum emission at 485 nm (REF.[87]) (FIG. 10e). After cleavage of the boronate pinacol ester by H_2O_2, a red shift from 485 to 585 nm in emission is observed, as a result of the ESIPT process of the generated compound **F**. Thus, probe **FB** could be used to map H_2O_2 changes in vascular smooth muscle cells under stimulation by phorbol myristate acetate using ratiometric imaging. Moreover, irradiation of compound **F** at 405 nm (or two-photon irradiation at 800 nm)

enables the release of carbon monoxide as a therapeutic agent in a photo-controllable manner[88]. Such sequential activation processes of **FB** make it possible to visualize H_2O_2 fluctuations in the blood vessels of zebrafish and observe the vasodilation effects of CO in the treatment of angiotensin II-induced hypertension.

Conclusions and outlook

In this Review, we have summarized the development of dual-locked probes for bioimaging in living systems. We focused on the different chemical structures that have been used to generate dual-locked probes with bespoke optical properties and to facilitate their specific activation towards different biomarkers. We present design strategies (FIGS 1–10) used for the construction of dual-locked probes. The design strategies are classified based on changes in optical outputs and the number of reaction sites that the probe contains. Interestingly, only one practical example is available for the dual-locked systems of FIGS 7a,8c,10d. As such, these systems represent potential areas for future development. A word of caution is appropriate for the development and application of systems like those highlighted in FIG. 7, where

two probes are required. Practical problems may arise during application, as a result of differences in permeability, incubation time and distribution of the probes within the cells or live animals when compared with systems developed using a unimolecular dual-locked probe (FIG. 6). In addition, two-probe systems can potentially result in reduced biocompatibility compared with unimolecular-probe systems.

Compared with single-factor activatable probes, dual-locked probes with a sequential strategy to generate an optical response (FIGS 1,2) and the 'AND'-based probes (FIGS 6,7) share the advantages of avoiding nonspecific activation and 'false positive' results in complex environments[89]. Nevertheless, an area requiring improvement for many dual-locked systems is the elimination of potential crosstalk. For example, the use of two similar fluorescence channels for discrimination of the duplex (FIG. 4) can result in emission crosstalk during bioimaging. In order to circumvent this problem, differentiation using two independent optical channels or the combination of chemiluminescence with fluorescence is required (FIG. 5b). Therefore, it is important that researchers explore such dual-locked systems because they pave the way for crosstalk-free sensing. For example, probe **ADR** bearing β-cyclodextrin produces chemiluminescence and NIR fluorescence 'turn-on' signals towards $O_2^{\cdot-}$ and NAG, respectively, in the kidneys.

Both FRET and ESIPT are important fluorescence mechanisms. FRET is a common strategy used for the construction of dual-locked probes (FIG. 8), while ESIPT is a scarcer strategy (FIG. 9b). Unlike other reaction-based dual-locked probes, ESIPT probe **3-HF-OMe** incorporates 'host–guest' sensing, where Aβ peptide aggregates serve as host matrix (FIG. 9). Given the versatility of ESIPT-based systems, we anticipate that, provided longer wavelength systems can be developed, dual-locked probes based on ESIPT will become more commonplace.

Prodrug systems combining drug delivery and fluorescence imaging illustrate the robustness of dual-locked systems for both sensing and chemotherapy[90]. We anticipate that such dual-locked systems may provide a deeper understanding of the biological influence of drugs during therapy. For example, the two cancer biomarkers of acidity and GSH activate **P(Cy-S-CPT)** and trigger the release of the anticancer drug CPT (FIG. 9d).

A commonly used locking group discussed in this Review is the boronate pinacol ester. It is well known that boronate pinacol esters are more sensitive to reaction with $ONOO^-$ than H_2O_2 (REF.[91]). And, yet, numerous boronate-based probes have been reported with either $ONOO^-$ or H_2O_2 selectivity. For example, it has been reported that **THP** and **FB** display good selectivity towards H_2O_2 over $ONOO^-$ (REFS[47,87]). In these examples, however, tests were performed with only a single concentration of $ONOO^-$, and, as such, a response to $ONOO^-$ at different concentrations cannot be ruled out. However, the response of **QM-B-CF**, **Mito-VH** and **FP-H$_2$O$_2$-NO** probes towards $ONOO^-$ was not reported[25,42,61]. In the case of **Pinkment-OAc**, we made it clear that the probe could not be used for the detection of $ONOO^-$ AND esterase, as the probe was activated by just $ONOO^-$ to generate a fluorescent product (cleavage of both the boronic ester and phenyl acetate by $ONOO^-$)[92]. As such, a great deal of future confusion could be avoided if, when the boronate pinacol ester group is used to develop either dual or single 'locked' probes, a full evaluation of concentration-dependent and time-dependent reactivity towards both H_2O_2 and $ONOO^-$ is performed.

In summary, we have highlighted the clear advantages in selectivity provided by dual-locked probes for disease diagnosis, monitoring and treatment. With the advancement and convergence of chemistry, biology and medicine, we anticipate that more and more dual-locked probes will be developed, with key applications in either fundamental biology or translational medicine.

Published online: 20 May 2021

1. Rudin, M. & Weissleder, R. Molecular imaging in drug discovery and development. *Nat. Rev. Drug Discov.* **2**, 123–131 (2003).
2. Hong, G., Antaris, A. L. & Dai, H. Near-infrared fluorophores for biomedical imaging. *Nat. Biomed. Eng.* **1**, 0010 (2017).
3. Schnermann, M. J. Chemical biology: Organic dyes for deep bioimaging. *Nature* **551**, 176–177 (2017).
4. Zhang, R. R. et al. Beyond the margins: real-time detection of cancer using targeted fluorophores. *Nat. Rev. Clin. Oncol.* **14**, 347–364 (2017).
5. Domaille, D. W., Que, E. L. & Chang, C. J. Synthetic fluorescent sensors for studying the cell biology of metals. *Nat. Chem. Biol.* **4**, 168–175 (2008).
6. Huang, J., Li, J., Lyu, Y., Miao, Q. & Pu, K. Molecular optical imaging probes for early diagnosis of drug-induced acute kidney injury. *Nat. Mater.* **18**, 1133–1143 (2019).
7. Huang, J. & Pu, K. Near-infrared fluorescent molecular probes for imaging and diagnosis of nephro-urological diseases. *Chem. Sci.* **12**, 3379–3392 (2021).
8. Zhang, J., Campbell, R. E., Ting, A. Y. & Tsien, R. Y. Creating new fluorescent probes for cell biology. *Nat. Rev. Mol. Cell Biol.* **3**, 906–918 (2002).
9. Thomas, J. A. Optical imaging probes for biomolecules: an introductory perspective. *Chem. Soc. Rev.* **44**, 4494–4500 (2015).
10. Chan, J., Dodani, S. C. & Chang, C. J. Reaction-based small-molecule fluorescent probes for chemoselective bioimaging. *Nat. Chem.* **4**, 973–984 (2012).
11. Wu, L. et al. Reaction-based fluorescent probes for the detection and imaging of reactive oxygen, nitrogen, and sulfur species. *Acc. Chem. Res.* **52**, 2582–2597 (2019).
12. Fernández-Suárez, M. & Ting, A. Y. Fluorescent probes for super-resolution imaging in living cells. *Nat. Rev. Mol. Cell Biol.* **9**, 929–943 (2008).
13. Cañeque, T., Müller, S. & Rodriguez, R. Visualizing biologically active small molecules in cells using click chemistry. *Nat. Rev. Chem.* **2**, 202–215 (2018).
14. Jiang, Y. & Pu, K. Multimodal biophotonics of semiconducting polymer nanoparticles. *Acc. Chem. Res.* **51**, 1840–1849 (2018).
15. Miao, Q. & Pu, K. Organic semiconducting agents for deep-tissue molecular imaging: second near-infrared fluorescence, self-luminescence, and photoacoustics. *Adv. Mater.* **30**, 1801778 (2018).
16. Huang, J. & Pu, K. Activatable molecular probes for second near-infrared fluorescence, chemiluminescence, and photoacoustic imaging. *Angew. Chem. Int. Ed.* **59**, 11717–11731 (2020).
17. Rout, B., Milko, P., Iron, M. A., Motiei, L. & Margulies, D. Authorizing multiple chemical passwords by a combinatorial molecular keypad lock. *J. Am. Chem. Soc.* **135**, 15330–15333 (2013).
18. de Silva, A. P., Gunaratne, N. H. Q. & McCoy, C. P. A molecular photoionic AND gate based on fluorescent signalling. *Nature* **364**, 42–44 (1993).
19. Erbas-Cakmak, S. et al. Molecular logic gates: the past, present and future. *Chem. Soc. Rev.* **47**, 2228–2248 (2018).
20. Kolanowski, J. L., Liu, F. & New, E. J. Fluorescent probes for the simultaneous detection of multiple analytes in biology. *Chem. Soc. Rev.* **47**, 195–208 (2018).
21. Huang, J. et al. A renal-clearable duplex optical reporter for real-time imaging of contrast-induced acute kidney injury. *Angew. Chem. Int. Ed.* **58**, 17796–17804 (2019).
22. Liu, Y. et al. A "Double-Locked" and enzyme-activated molecular probe for accurate bioimaging and hepatopathy differentiation. *Chem. Sci.* **10**, 10931–10936 (2019).
23. Cheng, P. et al. Unimolecular chemo-fluoro-luminescent reporter for crosstalk-free duplex imaging of hepatotoxicity. *J. Am. Chem. Soc.* **141**, 10581–10584 (2019).
24. Miao, Q. et al. Molecular afterglow imaging with bright, biodegradable polymer nanoparticles. *Nat. Biotechnol.* **35**, 1102–1110 (2017).
25. Zhang, Y. et al. A sequential dual-lock strategy for photoactivatable chemiluminescent probes enabling bright duplex optical imaging. *Angew. Chem. Int. Ed.* **59**, 9059–9066 (2020).
26. He, S., Xie, C., Jiang, Y. & Pu, K. An organic afterglow protheranostic nanoassembly. *Adv. Mater.* **31**, 1902672 (2019).
27. Goldberg, J. M. et al. Photoactivatable sensors for detecting mobile zinc. *J. Am. Chem. Soc.* **140**, 2020–2023 (2018).
28. Halabi, E. A., Thiel, Z., Trapp, N., Pinotsi, D. & Rivera-Fuentes, P. A photoactivatable probe for super-resolution imaging of enzymatic activity in live cells. *J. Am. Chem. Soc.* **139**, 13200–13207 (2017).

REVIEWS

29. Thiel, Z. & Rivera-Fuentes, P. Single-molecule imaging of active mitochondrial nitroreductases using a photo-crosslinking fluorescent sensor. *Angew. Chem. Int. Ed.* **58**, 11474–11478 (2019).

30. Liu, C. et al. "Dual-key-and-lock" ruthenium complex probe for lysosomal formaldehyde in cancer cells and tumors. *J. Am. Chem. Soc.* **141**, 8462–8472 (2019).

31. Jiang, X.-J. & Ng, D. K. P. Sequential logic operations with a molecular keypad lock with four inputs and dual fluorescence outputs. *Angew. Chem. Int. Ed.* **53**, 10481–10484 (2014).

32. Tour, O. et al. Calcium Green FlAsH as a genetically targeted small-molecule calcium indicator. *Nat. Chem. Biol.* **3**, 423–431 (2007).

33. Griffin, B. A., Adams, S. R. & Tsien, R. Y. Specific covalent labeling of recombinant protein molecules inside live cells. *Science* **281**, 269–272 (1998).

34. Adams, S. R. et al. New biarsenical ligands and tetracysteine motifs for protein labeling in vitro and in vivo: synthesis and biological applications. *J. Am. Chem. Soc.* **124**, 6063–6076 (2002).

35. Dai, T. et al. A fluorogenic trehalose probe for tracking phagocytosed *Mycobacterium tuberculosis*. *J. Am. Chem. Soc.* **142**, 15259–15264 (2020).

36. Cheng, Y. et al. Rapid and specific labeling of single live *Mycobacterium tuberculosis* with a dual-targeting fluorogenic probe. *Sci. Transl Med.* **10**, eaar4470 (2018).

37. Fernandez, A., Thompson, E. J., Pollard, J. W., Kitamura, T. & Vendrell, M. A fluorescent activatable AND-gate chemokine CCL2 enables in vivo detection of metastasis-associated macrophages. *Angew. Chem. Int. Ed.* **58**, 16894–16898 (2019).

38. Dröge, W. Free radicals in the physiological control of cell function. *Physiol. Rev.* **82**, 47–95 (2002).

39. Zhang, R. et al. Real-time discrimination and versatile profiling of spontaneous reactive oxygen species in living organisms with a single fluorescent probe. *J. Am. Chem. Soc.* **138**, 3769–3778 (2016).

40. Li, H. et al. Ferroptosis accompanied by •OH generation and cytoplasmic viscosity increase revealed via dual-functional fluorescence probe. *J. Am. Chem. Soc.* **141**, 18301–18307 (2019).

41. Li, S.-J. et al. A dual-response fluorescent probe for the detection of viscosity and H_2S and its application in studying their cross-talk influence in mitochondria. *Anal. Chem.* **90**, 9418–9425 (2018).

42. Ren, M. et al. Single fluorescent probe for dual-imaging viscosity and H_2O_2 in mitochondria with different fluorescence signals in living cells. *Anal. Chem.* **89**, 552–555 (2017).

43. Wang, F. et al. A dual-response BODIPY-based fluorescent probe for the discrimination of glutathione from cystein and homocystein. *Chem. Sci.* **6**, 2584–2589 (2014).

44. Yue, Y. et al. Dual-site fluorescent probe for visualizing the metabolism of Cys in living cells. *J. Am. Chem. Soc.* **139**, 3181–3185 (2017).

45. Wu, M.-Y., Wang, Y., Liu, Y.-H. & Yu, X.-Q. Dual-site lysosome-targeted fluorescent probe for separate detection of endogenous biothiols and SO_2 in living cells. *J. Mater. Chem. B* **6**, 4232–4238 (2018).

46. Yuan, Y. et al. Light-up probe based on AIEgens: dual signal turn-on for caspase cascade activation monitoring. *Chem. Sci.* **8**, 2723–2728 (2017).

47. Wu, Z., Liu, M., Liu, Z. & Tian, Y. Real-time imaging and simultaneous quantification of mitochondrial H_2O_2 and ATP in neurons with a single two-photon fluorescence-lifetime-based probe. *J. Am. Chem. Soc.* **142**, 7532–7541 (2020).

48. Shuhendler, A. J., Pu, K., Cui, L., Uetrecht, J. P. & Rao, J. Real-time imaging of oxidative and nitrosative stress in the liver of live animals for drug-toxicity testing. *Nat. Biotechnol.* **32**, 373–380 (2014).

49. Zhang, C. et al. Dual-biomarker-triggered fluorescence probes for differentiating cancer cells and revealing synergistic antioxidant effects under oxidative stress. *Chem. Sci.* **10**, 1945–1952 (2019).

50. Sedgwick, A. C. et al. The development of a novel AND logic based fluorescence probe for the detection of peroxynitrite and GSH. *Chem. Sci.* **9**, 3672–3676 (2018).

51. Wu, L. et al. ESIPT-based fluorescence probe for the rapid detection of peroxynitrite 'AND' biological thiols. *Chem. Commun.* **54**, 11336–11339 (2018).

52. Odyniec, M. L. et al. 'AND'-based fluorescence scaffold for the detection of ROS/RNS and a second analyte. *Chem. Commun.* **54**, 8466–8469 (2018).

53. Droumaguet, C. L., Wang, C. & Wang, Q. Fluorogenic click reaction. *Chem. Soc. Rev.* **39**, 1233–1239 (2010).

54. Zhou, Z. & Fahrni, C. J. A fluorogenic probe for the copper(I)-catalyzed azide–alkyne ligation reaction: modulation of the fluorescence emission via $^3(n,\pi^*)–^1(\pi,\pi^*)$ inversion. *J. Am. Chem. Soc.* **126**, 8862–8863 (2004).

55. Liu, G. et al. Doubly caged linker for AND-type fluorogenic construction of protein/antibody bioconjugates and in situ quantification. *Angew. Chem. Int. Ed.* **56** (2017).

56. Yi, L. & Xi, Z. Thiolysis of NBD-based dyes for colorimetric and fluorescence detection of H_2S and biothiols: design and biological applications. *Org. Biomol. Chem.* **15**, 3828–3839 (2017).

57. Ong, W., Yang, Y., Cruciano, A. C. & McCarley, R. L. Redox-triggered contents release from liposomes. *J. Am. Chem. Soc.* **130**, 14739–14744 (2008).

58. Van de Bittner, G. C., Dubikovskaya, E. A., Bertozzi, C. R. & Chang, C. J. In vivo imaging of hydrogen peroxide production in a murine tumor model with a chemoselective bioluminescent reporter. *Proc. Natl Acad. Sci. USA* **107**, 21316–21321 (2010).

59. Van de Bittner, G. C., Bertozzi, C. R. & Chang, C. J. Strategy for dual-analyte luciferin imaging: in vivo bioluminescence detection of hydrogen peroxide and caspase activity in a murine model of acute inflammation. *J. Am. Chem. Soc.* **135**, 1783–1795 (2013).

60. Wu, L. et al. Förster resonance energy transfer (FRET)-based small-molecule sensors and imaging agents. *Chem. Soc. Rev.* **49**, 5110–5139 (2020).

61. Yuan, L., Lin, W., Xie, Y., Chen, B. & Zhu, S. Single fluorescent probe responds to H_2O_2, NO, and H_2O_2/NO with three different sets of fluorescence signals. *J. Am. Chem. Soc.* **134**, 1305–1315 (2012).

62. Ou, P. et al. Gasotransmitter regulation of phosphatase activity in live cells studied by three-channel imaging correlation. *Angew. Chem. Int. Ed.* **58**, 2261–2265 (2019).

63. Zhang, P. et al. A logic gate-based fluorescent sensor for detecting H_2S and NO in aqueous media and inside live cells. *Chem. Commun.* **51**, 4414–4416 (2015).

64. Chen, W. et al. A single fluorescent probe to visualize hydrogen sulfide and hydrogen polysulfides with different fluorescence signals. *Angew. Chem. Int. Ed.* **55**, 9993–9996 (2016).

65. Kourtis, N., Nikoletopoulou, V. & Tavernarakis, N. Small heat-shock proteins protect from heat-stroke-associated neurodegeneration. *Nature* **490**, 213–218 (2012).

66. Zhang, W. et al. Heat stroke in cell tissues related to sulfur dioxide level is precisely monitored by light-controlled fluorescent probes. *J. Am. Chem. Soc.* **142**, 3262–3268 (2020).

67. Sedgwick, A. C. et al. Excited-state intramolecular proton-transfer (ESIPT) based fluorescence sensors and imaging agents. *Chem. Soc. Rev.* **47**, 8842–8880 (2018).

68. Zhang, G., Shuang, S., Dong, C. & Pan, J. Study on the interaction of methylene blue with cyclodextrin derivatives by absorption and fluorescence spectroscopy. *Spectrochim. Acta A* **59**, 2935–2941 (2003).

69. Florea, M. & Nau, W. M. Implementation of anion-receptor macrocycles in supramolecular tandem assays for enzymes involving nucleotides as substrates, products, and cofactors. *Org. Biomol. Chem.* **8**, 1033–1039 (2010).

70. Sedgwick, A. C. et al. An ESIPT probe for the ratiometric imaging of peroxynitrite facilitated by binding to Aβ-aggregates. *J. Am. Chem. Soc.* **140**, 14267–14271 (2018).

71. Yu, F., Gao, M., Li, M. & Chen, L. A dual response near-infrared fluorescent probe for hydrogen polysulfides and superoxide anion detection in cells and in vivo. *Biomaterials* **63**, 93–101 (2015).

72. Gao, M., Yu, F., Chen, H. & Chen, L. Near-infrared fluorescent probe for imaging mitochondrial hydrogen polysulfides in living cells and in vivo. *Anal. Chem.* **87**, 3631–3638 (2015).

73. Liu, C. et al. Rational design and bioimaging applications of highly selective fluorescence probes for hydrogen polysulfides. *J. Am. Chem. Soc.* **136**, 7257–7260 (2014).

74. Lee, M. H. et al. Fluorogenic reaction-based prodrug conjugates as targeted cancer theranostics. *Chem. Soc. Rev.* **47**, 28–52 (2018).

75. Liu, Z. et al. A reversible fluorescent probe for real-time quantitative monitoring of cellular glutathione. *Angew. Chem. Int. Ed.* **56**, 5812–5816 (2017).

76. Yan, C. et al. A sequence-activated AND logic dual-channel fluorescent probe for tracking programmable drug release. *Chem. Sci.* **9**, 6176–6182 (2018).

77. Kojima, H. et al. Fluorescent indicators for nitric oxide based on rhodamine chromophore. *Tetrahedron Lett.* **41**, 69–72 (2000).

78. Gabe, Y., Urano, Y., Kikuchi, K., Kojima, H. & Nagano, T. Highly sensitive fluorescence probes for nitric oxide based on boron dipyrromethene chromophore-rational design of potentially useful bioimaging fluorescence probe. *J. Am. Chem. Soc.* **126**, 3357–3367 (2004).

79. Sasaki, E. et al. Highly sensitive near-infrared fluorescent probes for nitric oxide and their application to isolated organs. *J. Am. Chem. Soc.* **127**, 3684–3685 (2005).

80. Sun, Y.-Q. et al. A mitochondria-targetable fluorescent probe for dual-channel NO imaging assisted by intracellular cysteine and glutathione. *J. Am. Chem. Soc.* **136**, 12520–12523 (2014).

81. Ye, X., Rubakhin, S. S. & Sweedler, J. V. Simultaneous nitric oxide and dehydroascorbic acid imaging by combining diaminofluoresceins and diaminorhodamines. *J. Neurosci. Methods* **168**, 373–382 (2008).

82. Zhang, X. et al. Interfering with nitric oxide measurements 4,5-diaminofluorescein reacts with dehydroascorbic acid and ascorbic acid. *J. Biol. Chem.* **277**, 48472–48478 (2002).

83. Wang, T., Douglass, E. F., Fitzgerald, K. J. & Spiegel, D. A. A "turn-on" fluorescent sensor for methylglyoxal. *J. Am. Chem. Soc.* **135**, 12429–12433 (2013).

84. Katritzky, A. R. et al. Synthesis of coumarin conjugates of biological thiols for fluorescent detection and estimation. *Synthesis* **9**, 1494–1500 (2011).

85. Karthik, S. et al. Photoresponsive coumarin-tethered multifunctional magnetic nanoparticles for release of anticancer drug. *ACS Appl. Mater. Interfaces* **5**, 5232–5238 (2013).

86. Biswas, S. et al. A dual-analyte probe: hypoxia activated nitric oxide detection with phototriggered drug release ability. *Chem. Commun.* **54**, 7940–7943 (2018).

87. Li, Y. et al. A two-photon H_2O_2-activated CO photoreleaser. *Angew. Chem. Int. Ed.* **57**, 12415–12419 (2018).

88. Anderson, S. N. et al. A structurally-tunable 3-hydroxyflavone motif for visible light-induced carbon monoxide-releasing molecules (CORMs). *ChemistryOpen* **4**, 590–594 (2015).

89. Teng, K.-X., Niu, L.-Y., Kang, Y.-F. & Yang, Q.-Z. Rational design of a "dual lock-and-key" supramolecular photosensitizer based on aromatic nucleophilic substitution for specific and enhanced photodynamic therapy. *Chem. Sci.* **11**, 9703–9711 (2020).

90. Lang, W. et al. Recent advances in construction of small molecule-based fluorophore-drug conjugates. *J. Pharm. Anal.* **10**, 434–443 (2020).

91. Sikora, A., Zielonka, J., Lopez, M., Joseph, J. & Kalyanaraman, B. Direct oxidation of boronates by peroxynitrite: mechanism and implications in fluorescence imaging of peroxynitrite. *Free Radic. Biol. Med.* **47**, 1401–1407 (2009).

92. Han, H.-H. et al. Protein encapsulation: a new approach for improving the capability of small-molecule fluorogenic probes. *Chem. Sci.* **11**, 1107–1113 (2020).